An Iterative Procedure for Multivariable Decentralized Robust Control using ETF ⋆

Egydio Tadeu Gomes Ramos * **George Acioli Júnior** **
Péricles Rezende Barros ** **José Sérgio da Rocha Neto** **

* *Post-Graduate Program in Electrical Engineering, Electrical Engineering Department, Federal University of Campina Grande, PB, (e-mail: egydio.ramos@ee.ufcg.edu.br).*
** *Electrical Engineering Department, Federal University of Campina Grande, PB, (e-mail: [georgeacioli, prbarros, zesergio]@dee.ufcg.edu.br).*

Abstract: In this paper, an iterative procedure is proposed to design decentralized robust controllers for multivariable systems, based on the effective transfer function (ETF). The uncertainties in the process are taken into account using the multiplicative model, represented by a weight transfer function matrix. An $\mathcal{H}_\infty$ optimization is applied to the ETF of each loop in order to obtain decentralized controllers that achieve robust stability and nominal performance. In the iterative procedure, the ETF is calculated and a weight is adjust to improve the performance of the system, in order to achieve better results. The procedure was validate with simulation studies and an experiment performed on a temperature process.

Keywords: process control, decentralized control, robust control.

1. INTRODUCTION

Many industrial systems are multi-input and multi-output (MIMO). They are subject to performance requirements and physical constraints. Due to the interactions between loops, the controller design is more complex than for a single-input and single-output (SISO) system. Furthermore, the models used to represent system dynamics are subject to uncertainties, caused by unmodelled dynamics or external disturbances. A robust controller can be designed to guarantee closed loop stability and performance of the system under influence of this uncertainties.

There are a variety of methods to design robust controllers for MIMO systems. They usually results in a $\mathcal{H}_\infty$ optimization problem (Mackenroth, 2004). However, the controllers in this case are centralized, which is undesirable in some applications. They are difficulty to maintain when compared to a simple structure like a decentralized controller.

In Rosinova (2012) and Karimi et al. (2016), linear matrix inequality (LMI) based techniques for decentralized robust control of systems with uncertainties represented by convex polytopes are proposed. This problem leads to unfeasible LMIs, which requires some constraints to approximate by feasible ones. Alternatively, iterative LMIs have been used to design multivariable PID controllers for linear time-invariant systems without delays (Lin et al., 2004) and with time delays (Belhaj and Boubaker, 2017).

The effective transfer function (ETF) is an approach to take account of the interactions between loops. The main advantage is that the MIMO system can be decoupled in a set of equivalent SISO loops. Some works have proposed iterative methods for decentralized control tuning using ETF. In Jin and Liu (2014), it is proposed a non-convex optimization problem to obtain optimal PI/PID controllers with specific robustness indexes. In Silva and Barros (2020) an iterative procedure is proposed to tune decentralized PID controllers using gain and phase margin specifications. However, there is no method where it is possible to include system uncertainties in the controller design.

In this paper, an iterative procedure is proposed to design decentralized robust controllers for MIMO process. The system uncertainty is represented by a set of transfer function matrices, using a multiplicative model. The aim is to obtain a controller that achieves robust performance, taken account of the interactions between loops by means of the ETF. At each iteration step, the performance and uncertainty weights are defined for the system. The controller is obtained by solving one $\mathcal{H}_\infty$ optimization problem for each loop.

This paper is organized as follows. In Section 2, the plant, controller and effective transfer function are defined. The $\mathcal{H}_\infty$ optimization problem is presented in Section 3. In Section 4, the iterative procedure is presented. In Sections 5 and 6, simulated and experimental studies are shown. The conclusions are discussed in Section 7.

2. PROBLEM STATEMENT

Consider a $n \times n$ MIMO system represented by a stable nominal transfer function matrix:

⋆ This work was supported by CNPq - Brazil.

$$\mathbf{G}(s) = \begin{bmatrix} G_{11}(s) & G_{12}(s) & \dots & G_{1n}(s) \\ G_{21}(s) & G_{22}(s) & \dots & G_{2n}(s) \\ \vdots & \vdots & \ddots & \vdots \\ G_{n1}(s) & G_{n2}(s) & \dots & G_{nn}(s) \end{bmatrix}, \quad (1)$$

where $G_{ij}(s)$ represents the nominal system dynamics between the jth input and the ith output.

It is assumed that the system may have uncertainties, which can be represented using the multiplicative model:

$$\tilde{\mathbf{G}}(s) = (\mathbf{I} + \Delta(s)\mathbf{W_2}(s))\,\mathbf{G}(s), \quad (2)$$

where $\tilde{\mathbf{G}}(s)$ is one model with uncertainty, $\Delta(s)$ is a variable and stable transfer function matrix which satisfies $\|\Delta\|_\infty < 1$, $\mathbf{W_2}(s)$ is a fixed and stable transfer function matrix, and $\mathbf{I}$ is the $n \times n$ identity matrix. From robust control theory, is known that the uncertainty can be fully characterized with a proper selection of $\mathbf{W_2}(s)$ (Skogestad and Postlethwaite, 2005).

The decentralized controller structure is given by:

$$\mathbf{C}(s) = \begin{bmatrix} C_1(s) & 0 & \dots & 0 \\ 0 & C_2(s) & \dots & 0 \\ \vdots & \vdots & \ddots & \vdots \\ 0 & 0 & \dots & C_n(s) \end{bmatrix}. \quad (3)$$

In Fig. 1 is presented the block diagram of the decentralized robust control problem, with the nominal plant $\mathbf{G}(s)$, controller $\mathbf{C}(s)$ and weights $\mathbf{W_2}(s)$ and $\mathbf{W_1}(s)$, which is the desired performance defined over the frequency domain (Mackenroth, 2004). The variables $\mathbf{y}$, $\mathbf{y_r}$, $\mathbf{e}$ and $\mathbf{u}$ are the measured outputs, setpoints, control errors and plant inputs, respectively. For the controller design, we define the error outputs $\mathbf{z_1} = \mathbf{W_1}(s)\mathbf{e} = \mathbf{W_1}(s)\mathbf{S}(s)\mathbf{y_r}$ and $\mathbf{z_2} = \mathbf{W_2}(s)\mathbf{y} = \mathbf{W_2}(s)\mathbf{T}(s)\mathbf{y_r}$, which are optimized in order to loopshape the sensitivity function $\mathbf{S}(s)$ and complementary sensitivity function $\mathbf{T}(s)$.

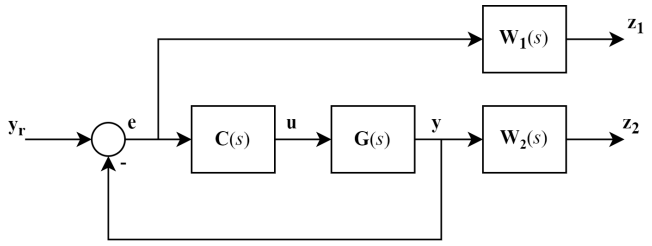

Figure 1. Block diagram of the robust control problem.

The problem consists in obtain $\mathbf{C}(s)$ such that the closed loop system is stable for any $\tilde{\mathbf{G}}(s)$ in the model, and guarantee the performance specified by $\mathbf{W_1}(s)$. In other words, the robust stability (4) and nominal performance (5) conditions must be met:

$$\|\mathbf{W_2}(s)\mathbf{T}(s)\|_\infty < 1, \quad (4)$$

$$\|\mathbf{W_1}(s)\mathbf{S}(s)\|_\infty < 1. \quad (5)$$

In some applications, it can be also possible to achieve robust performance:

$$\||\mathbf{W_2}(s)\mathbf{T}(s)| + |\mathbf{W_1}(s)\mathbf{S}(s)|\|_\infty < 1. \quad (6)$$

3. CONTROLLER DESIGN

In this section, the method for tuning the robust controller is presented. The $\mathcal{H}_\infty$ problem to be applied for the SISO subsystems is stated. Then a solution using linear matrix inequalities (LMIs) is presented.

3.1 $\mathcal{H}_\infty$ optimization

The design of a robust controller for the system is made using $\mathcal{H}_\infty$ optimization (Mackenroth, 2004). Based on structure represented in Fig. 1, for each loop, the generalized plant $\mathbf{P}_j(s)$ is the open loop transfer function matrix between inputs y_{rj}, u_j and outputs $\mathbf{z}_j = [z_{1j}\ z_{2j}]^T$, e_j, given by:

$$\mathbf{P}_j(s) = \begin{bmatrix} W_{1j}(s) & -W_{1j}(s)G_j(s) \\ 0 & W_{2j}(s)G_j(s) \\ 1 & -G_j(s) \end{bmatrix}. \quad (7)$$

The closed loop function between input y_{rj} and outputs $\mathbf{z}_j$, $\mathbf{F}_{zrj}(s)$, corresponds to the weighted sensitivity and complementary sensitivity functions:

$$\mathbf{F}_{zrj}(s) = \begin{bmatrix} W_{1j}(s)S(s) \\ W_{2j}(s)T(s) \end{bmatrix}. \quad (8)$$

To obtain the SISO robust controllers for each loop, the suboptimal $\mathcal{H}_\infty$ optimization is applied. The goal is to find a controller $C_j(s)$ such that:

$$\|\mathbf{F}_{zrj}\|_\infty < \gamma. \quad (9)$$

If it is possible to obtain a solution with $\gamma = 1$, then the closed loop is guaranteed to have robust stability and nominal performance. By doing a linear search of γ with lower values, it is also possible to achieve robust performance.

3.2 Formulation of optimization problem via LMIs

The $\mathcal{H}_\infty$ problem can be formulated as a linear matrix inequality (LMI) problem, by applying the Bounded Real Lemma (Dullerud and Paganini, 2010). An advantage of this approach despite classical Riccati equations method is that it is less restrictive concerning the model structure, so that it can be applied to more general cases. The solution can then efficiently be determined by using interior point method (Boyd et al., 1997).

Consider the state-space realizations of the generalized plant (10), assuming outputs $[z_{1j}\ z_{2j}]^T$ and y, and inputs r and e, as well as the controller (11) and closed loop models (12):

$$\mathbf{P}_j(s) = \left[\begin{array}{c|cc} \mathbf{A} & \mathbf{B_1} & \mathbf{B_2} \\ \hline \mathbf{C_1} & \mathbf{D_{11}} & \mathbf{D_{12}} \\ \mathbf{C_2} & \mathbf{D_{21}} & 0 \end{array}\right], \quad (10)$$

$$C_j(s) = \left[\begin{array}{c|c} \mathbf{A_K} & \mathbf{B_K} \\ \hline \mathbf{C_K} & \mathbf{D_K} \end{array}\right], \quad (11)$$

$$\mathbf{F}_{zrj}(s) = \left[\begin{array}{c|c} \mathbf{A_c} & \mathbf{B_c} \\ \hline \mathbf{C_c} & \mathbf{D_c} \end{array}\right]. \quad (12)$$

The controller design can be divided in two steps. First, LMIs (13) to (15) are solved to verify the existence of a controller who satisfies the optimization problem. Then, the controller can be obtained by solving (18).

There exists a controller such that $||\mathbf{F}_{zrj}||_\infty < \gamma$ if, and only if, exists two positive definite matrices $\mathbf{X}$ and $\mathbf{Y}$ who satisfies the following LMIs:

$$\begin{bmatrix} \mathbf{N_o} & \mathbf{0} \\ \mathbf{0} & \mathbf{I} \end{bmatrix}^T \begin{bmatrix} \mathbf{A}^T\mathbf{X} + \mathbf{X}\mathbf{A} & \mathbf{X}\mathbf{B_1} & \mathbf{C_1}^T \\ \mathbf{B_1}^T\mathbf{X} & -\gamma\mathbf{I} & \mathbf{D_{11}}^T \\ \mathbf{C_1} & \mathbf{D_{11}} & -\gamma\mathbf{I} \end{bmatrix} \begin{bmatrix} \mathbf{N_o} & \mathbf{0} \\ \mathbf{0} & \mathbf{I} \end{bmatrix} < \mathbf{0}, \quad (13)$$

$$\begin{bmatrix} \mathbf{N_c} & \mathbf{0} \\ \mathbf{0} & \mathbf{I} \end{bmatrix}^T \begin{bmatrix} \mathbf{A}\mathbf{Y} + \mathbf{Y}\mathbf{A}^T & \mathbf{Y}\mathbf{C_1}^T & \mathbf{B_1} \\ \mathbf{C_1}\mathbf{Y} & -\gamma\mathbf{I} & \mathbf{D_{11}} \\ \mathbf{B_1}^T & \mathbf{D_{11}}^T & -\gamma\mathbf{I} \end{bmatrix} \begin{bmatrix} \mathbf{N_c} & \mathbf{0} \\ \mathbf{0} & \mathbf{I} \end{bmatrix} < \mathbf{0}, \quad (14)$$

$$\begin{bmatrix} \mathbf{X} & \mathbf{I} \\ \mathbf{I} & \mathbf{Y} \end{bmatrix} \geq \mathbf{0}. \quad (15)$$

Here, $\mathbf{N_o}$ e $\mathbf{N_c}$ are full rank matrices such that:

$$\begin{aligned} \operatorname{Im} \mathbf{N_o} &= \ker \begin{bmatrix} \mathbf{C_2} & \mathbf{D_{21}} \end{bmatrix}, \\ \operatorname{Im} \mathbf{N_c} &= \ker \begin{bmatrix} \mathbf{B_2}^T & \mathbf{D_{12}}^T \end{bmatrix}, \end{aligned} \quad (16)$$

where $\operatorname{Im}(\cdot)$ and $\ker(\cdot)$ represents the image and null space of a matrix, respectively.

If there exists $\mathbf{X}$ and $\mathbf{Y}$ who satisfy (13) to (15), and a matrix $\mathbf{X_2}$ such that $\mathbf{X_2}\mathbf{X_2^T} = \mathbf{X} - \mathbf{Y^{-1}} \geq 0$, than $\mathbf{Z}$ is given by:

$$\mathbf{Z} = \begin{bmatrix} \mathbf{X} & \mathbf{X_2} \\ \mathbf{X_2}^T & \mathbf{I} \end{bmatrix}, \quad (17)$$

and the closed loop system matrices can be obtained by solving the following LMI:

$$\begin{bmatrix} \mathbf{A_c}^T\mathbf{Z} + \mathbf{Z}\mathbf{A_c} & \mathbf{Z}\mathbf{B_c} & \mathbf{C_c}^T \\ \mathbf{B_c}^T\mathbf{Z} & -\gamma^2\mathbf{I} & \mathbf{D_c}^T \\ \mathbf{C_c} & \mathbf{D_c} & -\mathbf{I} \end{bmatrix} < \mathbf{0}. \quad (18)$$

This way, the controller matrices in (11) can be obtained using linear relationships with $\mathbf{F}_{zrj}$. The proof of this statements can be found in Mackenroth (2004).

4. PROPOSED ITERATIVE PROCEDURE

The robust control method presented applied for SISO subsystems do not take into account the loop interactions. So, the guaranteed stability and robustness conditions are invalid in the MIMO decentralized control scenario. This way, the proposed methodology consists in obtain the controller for each loop using the effective trasfer function (ETF), so that the loop interactions can be take into account during solution.

4.1 Effective Transfer Function (ETF)

Consider the MIMO system $\mathbf{G}(s)$ in closed loop with the decentralized controller $\mathbf{C}(s)$. For the jth loop, the ETF (which will be called ETF_j) is defined as the SISO transfer function between output y_j and input u_j, when this loop is open and every other loop of the system is closed (Xiong and Cai, 2006).

In Silva and Barros (2020) is presented a procedure for obtaining the ETFs for each loop of a MIMO system. The diagram presented in Fig. 2 illustrate the structure of the system in order to apply the procedure. The controller outputs are denoted by $\mathbf{u}_c$ and the matrices Δ and $\overline{\Delta}$ are defined as following:

$$\Delta = \begin{bmatrix} \delta_1 & \dots & 0 \\ \vdots & \ddots & \vdots \\ 0 & \dots & \delta_n \end{bmatrix} \text{ and } \bar{\Delta} = \begin{bmatrix} \bar{\delta}_1 & \dots & 0 \\ \vdots & \ddots & \vdots \\ 0 & \dots & \overline{\delta_n} \end{bmatrix}.$$

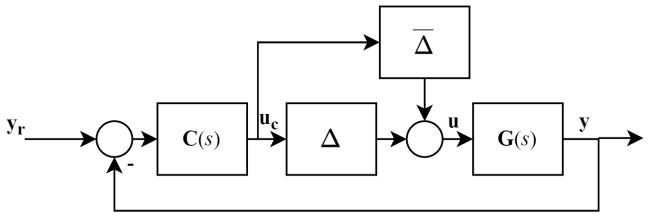

Figure 2. Structure to obtain ETFs in a MIMO system (Silva and Barros, 2020).

The values of $\delta_1, \cdots, \delta_n$ and $\bar{\delta}_1, \cdots, \bar{\delta}_n$ are adjusted depending of the loop which we want to obtained the ETF. For the jth loop, we set $\delta_j = 0$, $\delta_i = 1$, $\bar{\delta}_j = 1$ and $\bar{\delta}_i = 0$, where $i \in \mathrm{N}$, $1 \leq i \leq n$ and $i \neq j$.

According to Fig. 2, the following equations can be obtained:

$$\mathbf{y} = \mathbf{G}(s)\mathbf{u}, \quad (19)$$

$$\mathbf{y} = \mathbf{G}(s)\Delta\mathbf{u}_c + \mathbf{G}(s)\overline{\Delta}\mathbf{u}_c, \quad (20)$$

$$\mathbf{y} = \mathbf{G}(s)\Delta\mathbf{C}(s)(\mathbf{y}_r - \mathbf{y}) + \mathbf{G}(s)\overline{\Delta}\mathbf{u}_c. \quad (21)$$

The ETF is obtained by setting $\mathbf{y}_r = 0$, which results in:

$$\mathbf{y}(\mathbf{I} + \mathbf{G}(s)\Delta\mathbf{C}(s)) = \mathbf{G}(s)\overline{\Delta}\mathbf{u}_c, \quad (22)$$

$$\mathbf{y} = (\mathbf{I} + \mathbf{G}(s)\Delta\mathbf{C}(s))^{-1}\mathbf{G}(s)\overline{\Delta}\mathbf{u}_c, \quad (23)$$

After replace the matrices Δ and $\overline{\Delta}$ to obtain ETF_j, the entries of $\Delta\mathbf{C}$ and $\overline{\Delta}\mathbf{u}_c$ are:

$$\begin{aligned} &\Delta_{ii}C_{ii}(s) = C_i(s), \\ &\Delta_{jj}C_{jj}(s) = 0, \\ &\overline{\Delta}_{ii}u_{ci} = 0, \\ &\overline{\Delta}_{jj}u_{cj} = u_j. \end{aligned}$$

This way, only the jth loop is open, and the ETF can be obtained.

4.2 Algorithm

Given the $\mathbf{C}^{(0)}(s)$ initial controller which results in stability of closed loop, the goal is to find the ETFs for each loop with this controller. Then, $\mathcal{H}_\infty$ optimization is applied to each ETF to find a new controller $\mathbf{C}^{(1)}(s)$, based on desired specifications $\mathbf{W}_1$ and $\mathbf{W}_2$. This procedure can then be repeated a number of times to improve the controller performance specifications.

In Fig. 3 is presented a flowchart with the steps required to apply the algorithm. Some remarks concerning the procedure:

- obtain the ETF analytically for a system with uncertainties represented by (2) is not a trivial task, because of the difficulty in represent the ETF uncertainty in terms of the plant uncertainty. One alternative way is using an identification procedure to obtain a set of models of the ETF for each loop;
- the specification of weights $\mathbf{W}_1(s)$ can be done as presented in Mackenroth (2004). The transfer function must be stable, but a pole close to the origin may be included to guarantee integral effect. Parameters like gain and cut-off frequency are defined to loopshape the sensitivity function;

- specification of weights $\mathbf{W}_2(s)$ can be done as presented in Skogestad and Postlethwaite (2005). A set of models is needed to obtain the error of a transfer function $\tilde{\mathbf{G}}(s)$ in relation to the nominal model;
- the integral of absolute error (IAE) can be used to test the algorithm convergence. Because it accounts for the load disturbance rejection in controllers with integral action, it is a good measure of interaction between loops (Silva and Barros, 2020). It can be calculated by using time data of the closed loop system, using:

$$\text{IAE} = \int_0^\infty |e(t)|dt. \tag{24}$$

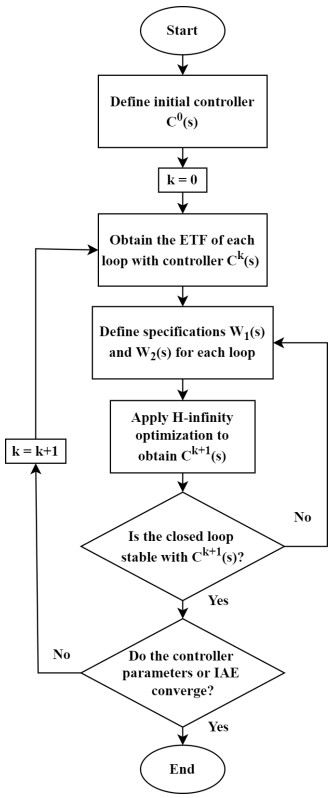

Figure 3. Flowchart of proposed iterative procedure.

5. SIMULATION RESULTS

In this section, the proposed procedure is evaluated at the Wood-Berry distillation column (Wood and Berry, 1973). The transfer matrix is:

$$\mathbf{G}_{WB}(s) = \begin{bmatrix} \dfrac{12.8e^{-s}}{16.7s+1} & \dfrac{-18.9e^{-3s}}{21s+1} \\ \dfrac{6.6e^{-7s}}{10.9s+1} & \dfrac{-19.4e^{-3s}}{14.4s+1} \end{bmatrix}. \tag{25}$$

For the design specifications, because the system is uncertainty free, $\mathbf{W}_2(s)$ was set to $\mathbf{0}$. The performance specification of each loop was defined as the following first order filter:

$$W_{1j}(s) = \frac{1}{S_\infty}\frac{s+\omega_c}{s+0.001\omega_c}, \tag{26}$$

where S_∞ is used to weight the sensitivity function gain at high frequencies and ω_c is the cut-off frequency. For the first iteration, the values were:

$$S_{\infty 1} = S_{\infty 1} = 10, \quad \omega_{c1} = 2\pi 0.4 \quad \text{and} \quad \omega_{c2} = 2\pi 0.1.$$

After three iterations, there was no more significant improvements in performance, so the procedure was stopped. The values of γ for each loop were $\gamma_1 = 0.449$ and $\gamma_2 = 0.134$ The obtained controller was:

$$C_1(s) = 1.075\frac{(s+2.03)(s+0.03)}{s(s+3.43)(s+0.04)},$$

$$C_2(s) = -0.120\frac{(s+0.68)(s+0.07)(s^2+0.56s+0.22)}{s(s+0.1)(s^2+1.10s+0.70)}.$$

The closed loop step response for each loop is presented in Fig. 4. The proposed controller is compared with the methods proposed by Chen and Seborg (2001) and Silva and Barros (2020). As can be seen, the application of proposed controller results in a faster response than the other, with less oscilation and smaller overshoot for loop 2.

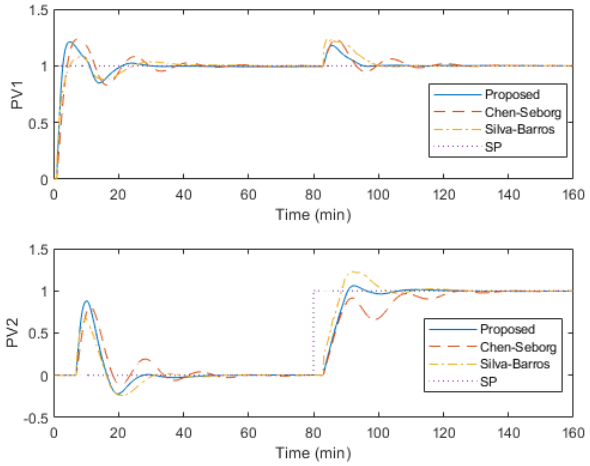

Figure 4. Step response for Wood-Berry process simulation.

To verify the interaction between loops, the IAE was computed to account the load disturbance rejection, whose values are presented in Table 1.

Table 1. IAE values calculated for step responses of Woody-Berry process.

Controller	Method	IAE
$C_1(s)$	Chen-Seborg	2.26
	Silva-Barros	2.43
	Proposed	1.63
$C_2(s)$	Chen-Seborg	7.70
	Silva-Barros	6.15
	Proposed	5.15

6. EXPERIMENTAL RESULTS

In this section, it is presented the application of proposed procedure to a MIMO temperature process. The system was proposed in Lima et al. (2018), and consists in two transistors and two temperature sensors. In Fig. 5 is presented a schematics with component disposition in the temperature module.

The inputs are duty cicles of PWM signals apllied to each transistors, while the outputs are the measured temperatures of each sensor. Because of constructive characteristics, the system is non linear and with highly coupled.

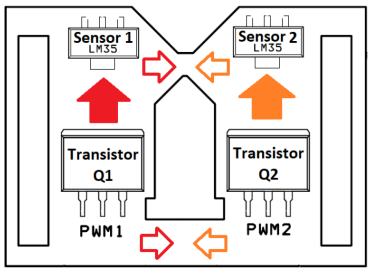

Figure 5. Temperature module schematic.

The initial controllers $C_1^0(s)$ and $C_2^0(s)$ used were:

$$C_1^0(s) = 0.07\frac{(s+0.072)(s+0.005)}{s(s+0.062)(s+0.043)},$$

$$C_2^0(s) = 0.06\frac{s+0.099)(s+0.006)}{s(s^2+0.085s+0.003)},$$

which results in a stable closed loop system, but poor performance.

Then, the ETF set of models for each loop was obtained by doing a identification of the system in different operation points. This was done by apllying a sequence of steps with the same amplitude in different operating points, as shown for the loop 1 in Fig. 6, where PV1 and PV2 are the temperatures of loop 1 and 2, respectively.

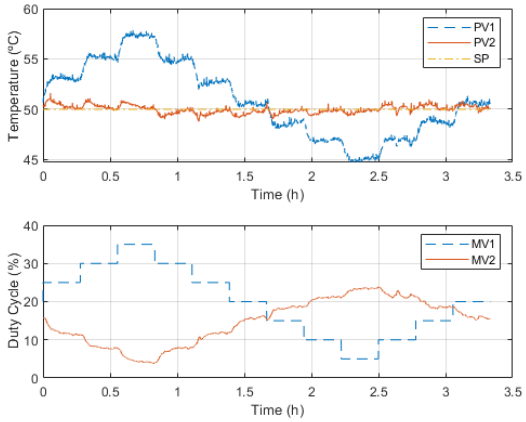

Figure 6. Step test to obtain the ETF set of models for loop 1.

For each step, the input and output data were used to estimate a set of models for the ETF. To account the observed overshoot in the curves, a second order transfer function was used, with the following structure:

$$\text{ETF}_j = \frac{K}{as+bs+1}e^{-sL} \tag{27}$$

where K is the gain, L the time delay, a and b are constants related with the poles. Using this procedure, a set of 12 models are obtained for each loop. The nominal model is obtained by take the mean value of each parameter in (27).

With the set of models, $\mathbf{W}_2(s)$ was obtained using the procedure in Skogestad and Postlethwaite (2005). The performance weight $\mathbf{W}_1(s)$ was defined using (26).

The IAE was calculated for the closed loop at each iteration to verify the load disturbance rejection, and the values of γ for each iteration. The values are presented in Table 2. Using the required performance leads to a controller with can achieve robust stability and nominal performance, but not robust performance. To achieve it, the performance weight needs to be very conservative, leading to poor results. After the third iteration, there was no notable improvement on the IAE, so the algorithm was stopped. The final controller transfer functions were:

$$C_1^3(s) = 0.710\frac{(s+0.272)(s+0.031)(s+0.023}{s(s+1.325)(s^2+0.105s+0.006)},$$

$$C_2^3(s) = 0.123\frac{s+0.162)(s^2+0.049s+0.001)}{s(s+0.126)(s^2+0.075s+0.005)}.$$

Table 2. IAE values calculated for the controllers of ETF for each iteration.

Controller	Iteration	IAE ($\times 10^3$)	γ
$C_1(s)$	1	3.86	0.825
	2	3.26	0.861
	3	2.89	0.928
$C_2(s)$	1	3.93	0.846
	2	2.61	0.932
	3	2.50	0.974

A closed loop experiment was performed using the decentralized controller obtained in the last iteration. A set of steps with amplitude of 2.5 $°C$ were applied to each loop individually. The goal was to evaluate the reference track in different operation points and the decoupling between loops. The result of this test for the loop 2 is presented by the time data shown in Fig. 7. It can be seen that the system follows the setpoint and the disturbance caused by coupling is zero in the steady-state.

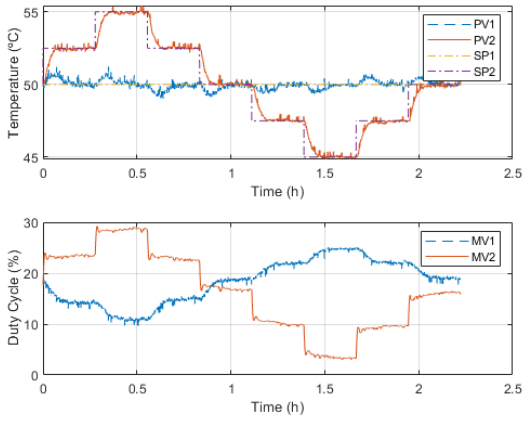

Figure 7. Closed loop experiment with setpoint change on loop 2, using the decentralized controller obtained in the last iteration.

To compare the performance in closed loop, two other controllers were tested. First was the initial decentralized controller $\mathbf{C}^0(s)$. Then, a centralized controller was designed by applying the $\mathcal{H}_\infty$ optimization to the full system, using suitable weights $\mathbf{W}_2(s)$ and $\mathbf{W}_1(s)$ to achieve robust stability and nominal performance.

In Figs. 8 and 9 are presented snapshots of one of the steps applied in each loop. The IAE was calculated for each case and is presented in Table 3. As expected, the centralized controller has the best performance in the decoupling, because of the off-diagonal terms in its transfer function

matrix. The final decentralized controller results in better performance in comparison with the initial.

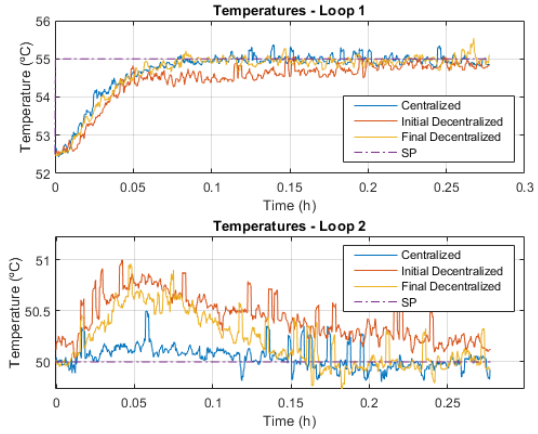

Figure 8. Closed loop experiment with setpoint change on loop 1 and comparison between controllers.

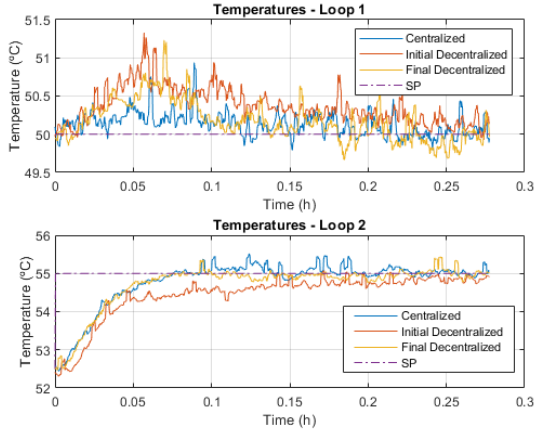

Figure 9. Closed loop experiment with setpoint change on loop 2 and comparison between controllers.

Table 3. IAE and γ values calculated for each iteration of the closed loop experiments.

Controller	Method	IAE ($\times 10^3$)
$C_1(s)$	Centralized	0.89
	Decentralized Initial	2.78
	Decentralized Final	1.71
$C_2(s)$	Centralized	1.31
	Decentralized Initial	2.26
	Decentralized Final	1.84

In the reference tracking the performance of both the centralized and decentralized final were approximately equal, even though the latter has a more simple structure. This was possible because the lesser complexity of control problem, which made possible to obtain a solution to $\mathcal{H}_\infty$ optimization with better performance weights $\mathbf{W}_1(s)$.

7. CONCLUSION

An iterative procedure was proposed to design decentralized robust controllers for MIMO systems. It takes the ETF to account for interaction between loops. The controller is obtained by applying the $\mathcal{H}_\infty$ optimization for each loop, using weights to account model uncertainties and desired performance. The methodology was validate with a simulation example and an experiment. In the simulations, it was verified the performance in comparison with other similar techniques. The application on the temperature module shown that good results can be achieved for decoupling and reference tracking.

As future work, it can be explored the analytical determination of the ETF for a system with uncertainties represented by a set of models, instead of using identification procedures at each iteration.

REFERENCES

Belhaj, W. and Boubaker, O. (2017). Mimo pi controllers for lti systems with multiple time delays based on ilmis and sensitivity functions. *Mathematical Problems in Engineering*, 2017.

Boyd, S., Ghaoui, L.E., Feron, E., and Balakrishnan, V. (1997). *Linear matrix inequalities in system and control theory*. Studies in Applied and Numerical Mathematics. Society for Industrial Mathematics.

Chen, D. and Seborg, D.E. (2001). Multiloop pi/pid controller design based on gershgorin bands. *Proceedings of the 2001 American Control Conference.*, 5, 4122–4127.

Dullerud, G.E. and Paganini, F. (2010). *A Course In Robust Control Theory*. Texts in Applied Mathematics. Springer, 1st ed. 2000. corr. 2nd printing edition.

Jin, Q. and Liu, Q. (2014). Multi-loop pi/pid controllers design for disturbance rejection based on non-parametric effective model and non-convex optimisation. *IET Control Theory & Applications*, 8(15), 1499–1512.

Karimi, A., Nicoletti, A., and Zhu, Y. (2016). Robust h-infinity controller design using frequency-domain data via convex optimization. *International Journal of Robust and Nonlinear Control*, 28.

Lima, A.B., Barros, P.R., and Acioli Junior, G. (2018). Módulo didático para ensino de teoria de controle. *Anais do XXII Congresso Brasileiro de Automática*, 1.

Lin, C., Wang, Q.G., and Lee, T.H. (2004). An improvement on multivariable pid controller design via iterative lmi approach. *Automatica*, 40(3), 519–525.

Mackenroth, U. (2004). *Robust Control Systems: Theory and Case Studies*. Springer-Verlag Berlin Heidelberg, 1 edition.

Rosinova, Danica; Vesely, V. (2012). Decentralized robust control of linear uncertain systems. *IFAC Proceedings Volumes*, 45, 412–417.

Silva, M.T. and Barros, P.R. (2020). An iterative procedure for tuning decentralized pid controllers based on effective open-loop process. *7th CoDIT*, 1, 813–818.

Skogestad, S. and Postlethwaite, I. (2005). *Multivariable Feedback Control: Analysis and Design*. Wiley-Interscience, 2 edition.

Wood, R. and Berry, M. (1973). Terminal composition control of a binary distillation column. *Chemical Engineering Science*, 28(9), 1707–1717.

Xiong, Q. and Cai, W. (2006). Effective transfer function method for decentralized control system design of multi-input multi-output processes. *Journal of Process Control*, 16(8), 773–784.